# EXPERIMENTAL COMPARISON OF TENSILE ARMOR WIRES USING STRAIN GAGES AND FIBER BRAGG GRATING TECHNIQUES

**Felipe Arêas Vargas**[1,2]
**Diogo Garcia Lopes**[1,2]
[1]GE Oil & Gas do Brasil LTDA - Rua Paulo Emídio Barbosa, 485 - Quadra 6.1(parte) -Módulo 10 - Parque tecnológico da UFRJ - Cidade Universitária, Ilha do Fundão – RJ – CEP21941-615
[2]PPEMM - Programa de Pós-Graduação em Engenharia Mecânica e Tecnologia de Materiais - CEFET/RJ - Av. Maracanã, 229 - Maracanã - RJ - CEP 20271-110 - Brazil
fel.varg@hotmail.com, diogo9021@yahoo.com.br

**Paulo Pedro Kenedi**
PPEMM - Programa de Pós-Graduação em Engenharia Mecânica e Tecnologia de Materiais - CEFET/RJ - Av. Maracanã, 229 - Maracanã - RJ - CEP 20271-110 - Brazil
pkenedi@cefet-rj.br

*Abstract. Flexible pipes, demanding intense technological development, are commonly used as a solution to explore ultra-deepwater oil fields. The structural complexity of flexible pipes is based on multiple independent layers of polymeric and metallic materials, each layer performing a specific function, e.g. the tensile armor wires, which provide the pipe's axial tension resistance. These layers need to be anchored into the end fitting during the assembly process. Currently, during manufacture it is necessary to submit the tensile armor wires to a folding/unfolding process, which generates high levels of plastic strain on the wires,which can therefore reduce the fatigue life of the flexible pipe in the field. In the comparison described in this paper, strain gages and fiber Bragg grating sensors were installed along the length of the tensile armor wires to measure the levels of strain occurring during the folding and unfolding process. This paper evaluates the high strains generated along the wire length during the standard folding/unfolding process and correlates the performance of both methods to assess high strain levels.*
*Keywords: Fiber Bragg grating, strain gages, high strain monitoring, flexible pipe, tensile armor layer.*

## 1. INTRODUCTION

With the growth of oil and gas exploration in ultra-deepwater, the use of flexible pipe has gained headway due to its good bending capacity related to its axial stiffness and structural integrity. Flexible pipes are used in many applications such as oil and gas production, water and gas injection, and fluid control services. Depending on the application, and for example in the case of top risers, flexible pipes can be subjected to high tension levels and fatigue loading (Xavier, 2009).

Flexible pipe has a structural complexity based on multiple independent layers of polymeric and metallic materials, each layer performing different and specific functions. Basically, polymeric layers provide a sealing function while metallic layers provide a structural function (Santos, 2008). The tensile armor layers provide the flexible pipe's tensile strength, and comprise two layers of carbon steel wires, helically wound in opposite directions. These layers are folded during the end fitting assembly process to allow access for sealing rings to be applied to underlying extruded polymer layers. The small curvature radius on the wires, necessary during end fitting, can generate high levels of plastic strain, which can result in residual stresses, reducing the fatigue life of the flexible pipe in the field (Sheldrake, 2008).

As these high strain levels are difficult to predict with accuracy, there is an interest in studying this background area in greater depth. Once the data is obtained, it will be possible to improve flexible pipe fatigue design, providing increasingly reliable design conditions. For the strain measurements in this work, the electrical extensometry method using strain gages and the optical extensometry method by Fiber Bragg Grating (FBG) were utilized.

The purpose of this work was to evaluate the strain levels in the areas of tensile armor wire defined by small curvature radius of the wire during the end fitting process, using both electrical and optical instrumentation techniques. In order to achieve a good approximation of real strain levels on the specimens, the tests were performed using a device that simulates the curvatures applied to a tensile armor wire.

## 2. CURVATURE DEVICE

A curvature device was developed to simulate the steps of the tensile armor bending during the end fitting process. The device consists of a former (introducing a specific radius), spider lock and a base (Lopes, 2013). Figure 1 shows a schematic drawing of the curvature device. The tests were carried out bending high carbon steel tensile armor until they were locked in the back position (in the spider lock), after which, the tensile armor was released from the back position and fixed on the base for the final configuration.
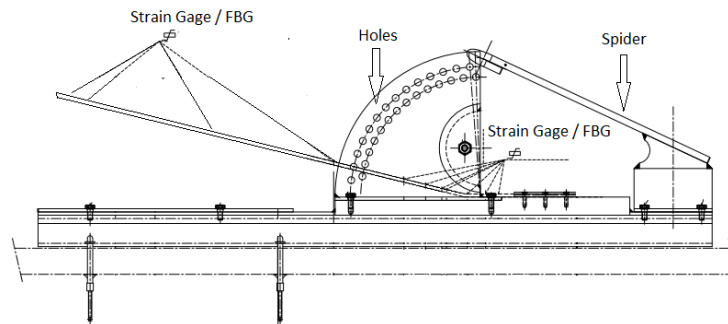


Figure 1 – Curvature device sketch. (Lopes, 2013)

## 3. EXPERIMENTAL METHODS

The tests were carried out using two different strain monitoring systems to evaluate the capacity for high strain level monitoring. A comparative assessment is presented describing the advantages and main characteristics of each method for this application.

### 3.1 Tests Using Strain Gages

The most common type of strain gage consists of an insulating flexible backing which supports a metallic foil pattern. Usually, the strain gage is bonded to the object by adhesive, such as cyanoacrylate or similar. When the object is deformed, the foil is also deformed causing its electrical resistance to change. This resistance change, usually measured using a Wheatstone bridge, is related to the strain by the quantity known as the gage factor ($GF$). The relationship between strains ($\varepsilon$) and electrical resistance variation ($\Delta R$) can be seen in Equation 3.1; the relationship between voltage output ($V_o$) and strains ($\varepsilon$) can be seen in Equation 3.2

$$\varepsilon = \frac{\Delta R}{R} \, GF \tag{3.1}$$

$$V_o \approx \left( \frac{GF}{4} \right) V_i \varepsilon \tag{3.2}$$

Where, $R$ is the strain gage resistance and $V_i$ is the voltage input.

Once the position of the strain gages had been determined, the process of installing them could begin. The first part of the process was to clean the tensile armor with a sandpaper grain size 200 finishing with a 400 grit sandpaper. Marks were then made on the sanded surface where the strain gages would be attached. A neutralizing agent (isopropanol) was used as the final part of the cleaning process. Lastly, the strain gages were bonded with Loctite 401 and connected to the Wheatstone bridge using a ¼ bridge, three-wire configuration (Lopes, 2013).

A total of 22 strain gages were bonded to the tensile armor, eleven on top of the tensile armor and eleven on the bottom of the tensile armor, coincident with those on top. Figure 1 shows the critical regions where the strain gages were bonded, some of which can also be seen in Figure 2.

Figure 2 – Strain gages bonded on tensile armor specimen.

Uniaxial strain gages manufactured by Kyowa were used, the main characteristics of which are shown in Table 1.

Table 1. Strain gages characteristics

| Strain Gage | | | | |
|---|---|---|---|---|
| Model | Base dimensions (mm) | Length (mm) | Resistence (Ω) | Maximum strain (%) |
| KFEL-2-120-C1-L30C3R | 8 x 4 | 2 | 120 | 10 |

For loggin, conditioning and storage of the strain data was used together, an acquisition controller, model 2122 CA and a signal conditioner, model 2164 Al from Lynx. After balancing, a calibration procedure, using a shunt calibration circuit, was performed. This circuit provides an imbalance known at the Wheatstone bridge, which is used to check gain. Also a preliminary test was performed with a known weight, as shown in Figure 3.



Figure 3 – Preliminary test. (Lopes, 2013)

The preliminary test was executed using a short tensile armor specimen. The strains were measured from a strain gage installed near the fixed end of cantilever beam, with a known mass at free end. The result are compared with an analytical model using Mechanics of Solids. The results showed little difference between the experimental and analytical calculation, with good results confirming the gain selection.

Figure 4 shows the strain experimental output of the preliminary test shown in Figure 3.
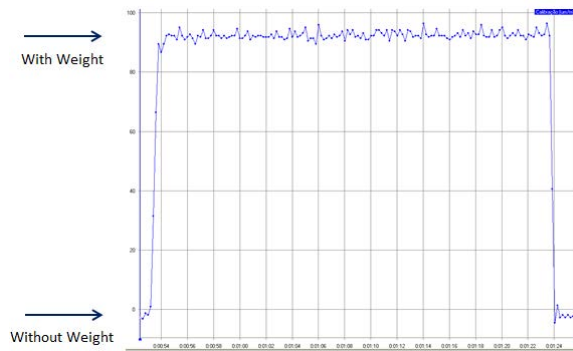


Figure 4 – Experimental output of Figure 3 preliminary test. (Lopes, 2013)

The main tests were performed in steps. Initially, the tensile armor was folded back and secured into the spider lock; the wire was then released allowing it spring-back elastically; finally the wire was bent back down and locked onto the Base, as shown in Figure 5.
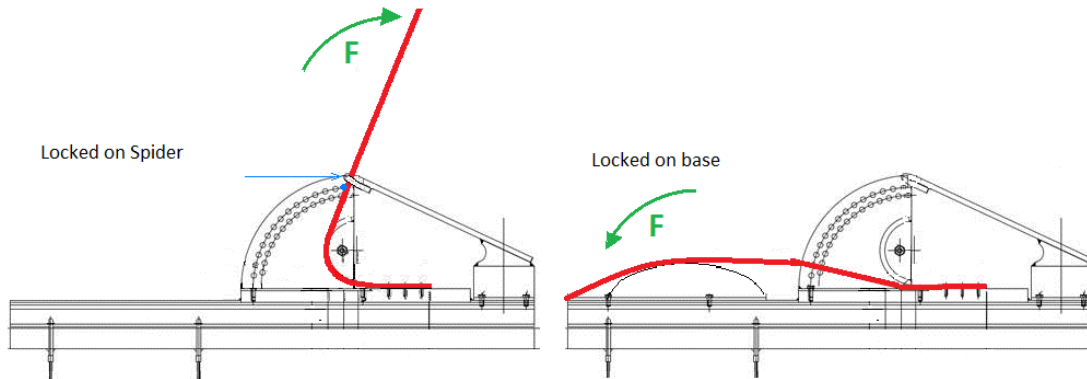


Figure 5 – Test steps. (Lopes, 2013)

The data acquisition was performed at 5Hz, at ambient temperature using a filter of 100Hz to bend the wires. Figures 6 and 7 present the test results by percentage, obtained from the division of the measured strains by the material yield strain limit, multiplied by 100. Figure 6 presents the results measured when the tensile armor was locked into the spider lock. Six tests were performed at each position along the tensile armor and it can be seen that the strains repeat at all points. It is noted that the strains measured at all points were relatively high with the most critical point achieving a peak strain of approximately 7.5 times greater than the yield strain. Furthermore, the strains showed a rapid and significant decrease away from the most critical region; this resultwas expected as the radius increases along the tensile armor. Finally, in those monitored areas more remote from the critical region the strains diminished to almost zero.
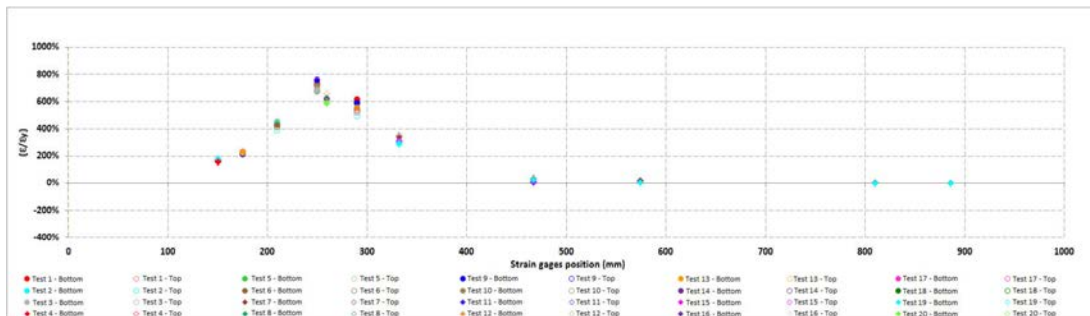


Figure 6 – Strains at back position - strain gages. (Lopes, 2013)

Figure 7 presents the results measured when the tensile armor was locked onto the base. Six tests were performed at each position along the tensile armor making it clear that the residual strains present in the tensile armor exceeded the yield strain limit at most locations, and at the most critical point reached approximately three times the yield strain. Again, the measured strains showed a significant decrease when moving from the critical region.
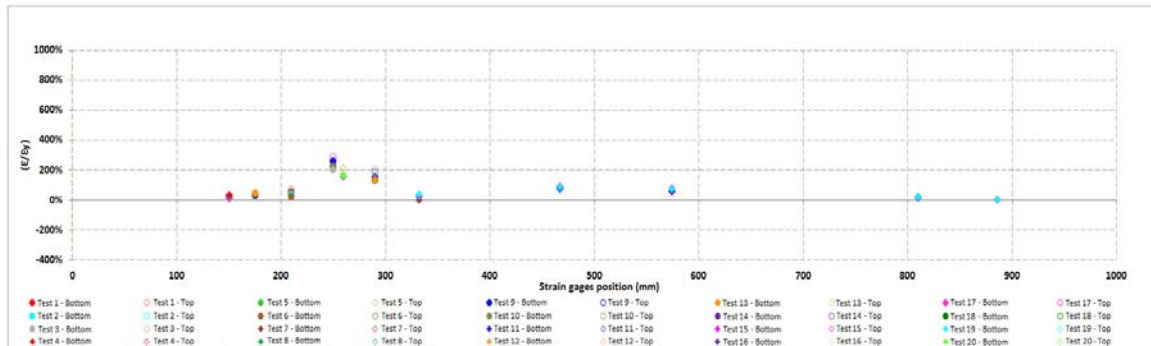


Figure 7 – Strains at base position - strain gages. (Lopes, 2013)

## 3.2 Tests Using FBG Sensors

FBG instrumentation is based on light transmitted between different locations in the form of beams. In many circumstances it is advantageous to transmit optical beams through dielectric conduits, rather than through free space. The technology for achieving this is known as guided-wave optics and in this case is the optical fiber.

An optical waveguide is a light conduit consisting of a slab, strip, or cylinder of dielectric material embedded in another dielectric material of lower refractive index. The light is transported through the inner medium without radiating into the surrounding medium.

For the purpose of this comparison, an optical fiber was used as the optical waveguide, comprising two concentric cylinders of low-loss dielectric material, such as glass. The optical fiber comprises core, cladding and buffer coating. The core is the central region of the optical fiber where the light is conducted; typically the diameter of the core is approximately 9 µm.The cladding around the core is made of dielectric material with a refractive index less than that of the core material. Covering the cladding is a buffer coating layer of polymeric material providing protection against mechanical damage (Cunha, 2007).

Because of the refractive index difference between the core and the cladding, this waveguide provides a good conduit for light rays. Figure 8 presents the optical fiber structural configuration.
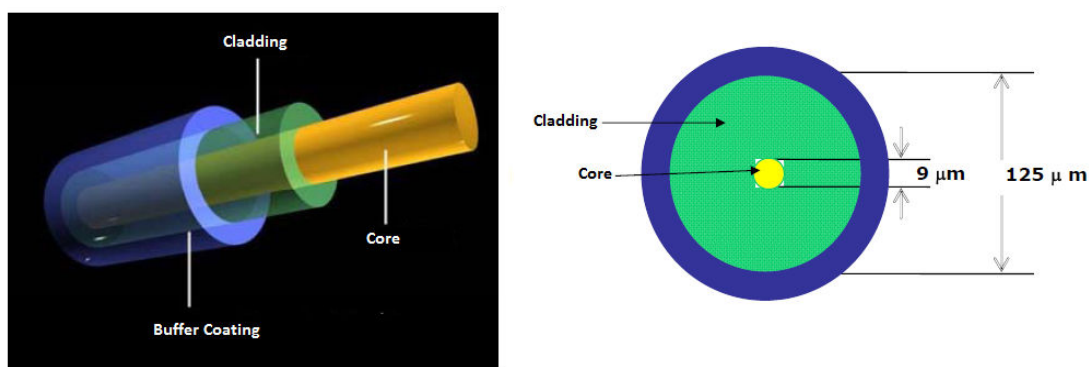


Figure 8 – Structural configuration of a monomode optical fiber. (Classroom notes, 2013)

The Bragg Grating itself is a section of fiber, or another fiber spliced into the first, in which a pattern of notched reflectors is cut or etched. The operation of a FBG sensor is based on a change of reflected wavelength, known as Bragg's wavelength, as a function of strain and temperature. Bragg's wavelength or reflected wavelength ($\lambda_B$) is related to the material's refractive index (n) and the band period ($\Lambda$), as shown in the following equation:

$$\lambda_B = 2n\Lambda \tag{3.3}$$

Felipe Arêas Vargas, Diogo Garcia Lopes and Paulo Pedro Kenedi
Experimental Comparison of Tensile Armor Wires using Strain Gages and Fiber Bragg Grating Techniques

Sensor systems involving such techniques usually work by conducting light into the optical fiber from a wideband spectral source, where part of the wavelength goes through the grating and the other is reflected, generating a peak in the spectrum with a small width. Figure 9 shows the circuit operation.
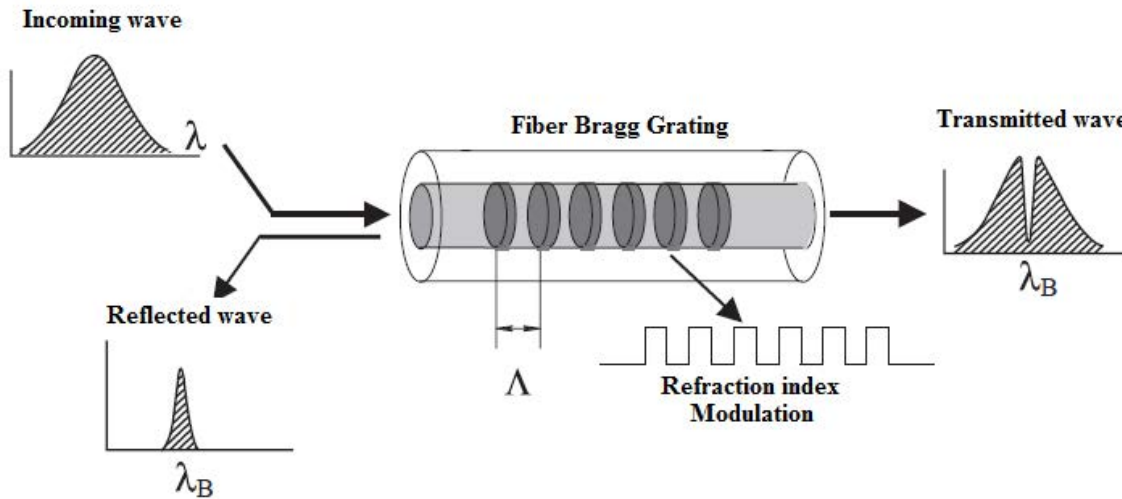


Figure 9 - Sensor operation principle based on the Bragg grating technique. (Quintero, 2005)

One of the most important functions of FBG sensors is the capacity of strain measurement and monitoring, which can be static, semi-static or dynamic (Grattan, 1995). When tension is applied in a FBG sensor a uniform linear variation of the modulation period occurs. Therefore, there is a reflected wavelength variation, which has a linear relation to applied strain based on equation 3.4 as follows:

$$\frac{\Delta \lambda_B}{\lambda_{B0}} = k \cdot \varepsilon + \alpha \cdot \Delta T \tag{3.4}$$

Where, $\Delta \lambda_B$ is the reflected wavelength variation, $\lambda_{B0}$ is the initial reflected wavelength i.e., without tension, k is the gage factor, usually 0.78, $\Delta T$ is the temperature variation in Kelvin and $\alpha$ is the refractive index variation.

Part $k \cdot \varepsilon$ of equation 3.4 describes the influence on the strain generated by the tension applied while part $\alpha \Delta T$ indicates the influence caused by temperature. Figure 10 shows how the reflected wavelength variation, measured when the FBG sensor is tensioned, occurs changing linearly with strain (Antunes, 2010).
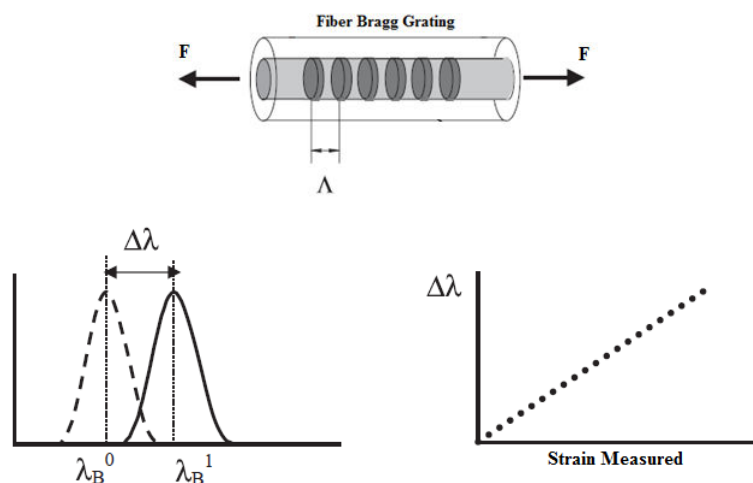


Figure 10 – Relation between applied tension, reflected wavelength variation and strain. (Quintero, 2005)

The FBG test sequence on the strain gage tests and the procedure to plot the graphs were performed identically.The only differences between the strain gage curvature device and the FBG curvature device were some additional precautions regarding their application to prevent the fiber from breaking during bending.

For the FBG instrumentation, high strain optical fibers were chosen to support the real strain applied in the test to avoid any sensor spectral loss. To optimize the data analysis, the instrumentation was used with one sensor per fiber, i.e., without multiplexing. Figure 11 presents the FBG sensor instrumentation.



Figure 11– FBG sensor instrumentation.

Figure 12 shows the strain results when the tensile armor was locked into the spider lock. Only one set of tests was performed at each position along the tensile armor and it can be seen that the strains repeated on the top and bottom sections. It is noted that the strains at all critical points were very high and at the most critical point, achieved approximately seven times the yield strain. The strains again show a significant decrease when moving from the most critical region. This result was expected as the radius increased along the tensile armor away from the critical area. Finally, remote from the critical region the strains were close to zero.
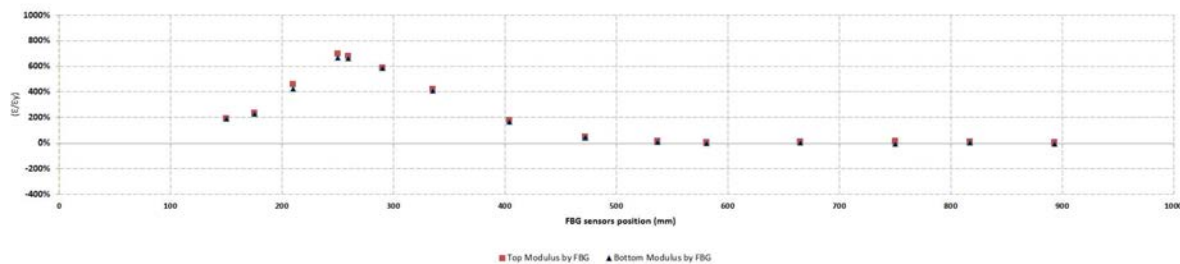


Figure 12 – Strains at back position, Bragg Grating. (Vargas, 2013)

Figure 13 shows the results when the tensile armor was locked onto the base. It can also be seen from Figure 12 that the strains repeated at the top and bottom sections. Only one set of tests was performed at each position along the tensile armor. It is clear that the residual strains present in the tensile armor exceeded the yield strain at almost every critical point, and that at the most critical point achieved approximately 2.5 times greater yield strain. The strains showed a significant decrease away from the most critical region.
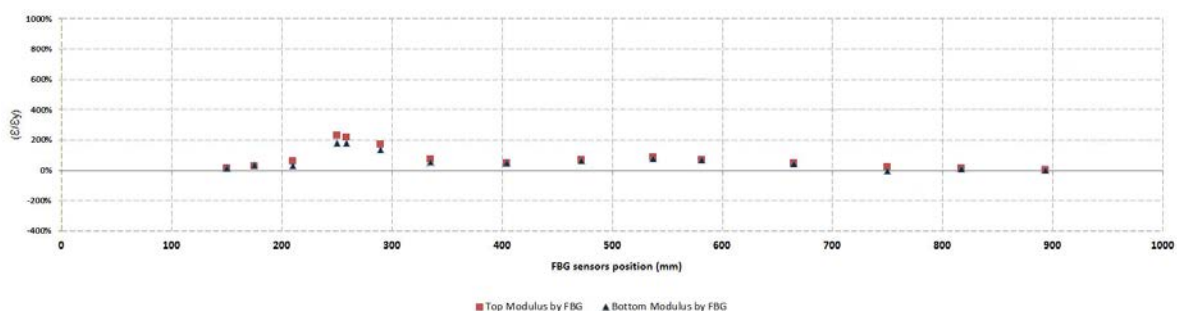


Figure13 – Strains at base position, Bragg Grating. (Vargas, 2013)

Felipe Arêas Vargas, Diogo Garcia Lopes and Paulo Pedro Kenedi
Experimental Comparison of Tensile Armor Wires using Strain Gages and Fiber Bragg Grating Techniques

## 4. COMPARISION BETWEEN STRAIN GAGES AND FBG TECHNIQUES

Figures 13 and 14 shows a direct comparison between these two different techniques. Also the principal advantages and disadvantages of both techniques are commented. Note that vertical axis of Figures 13 and 14 are obtained by the division of the measured strains by the material yield strain multiplied by 100.
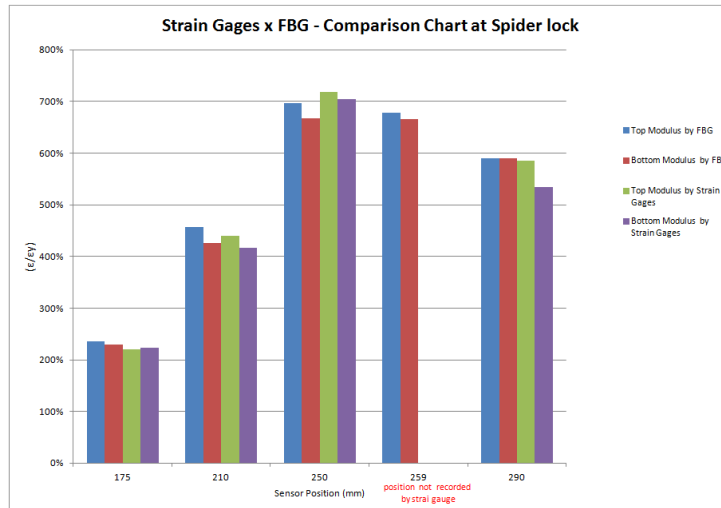


Figure 14 – Strain comparison between Strain Gage and FBG techniques at back position.
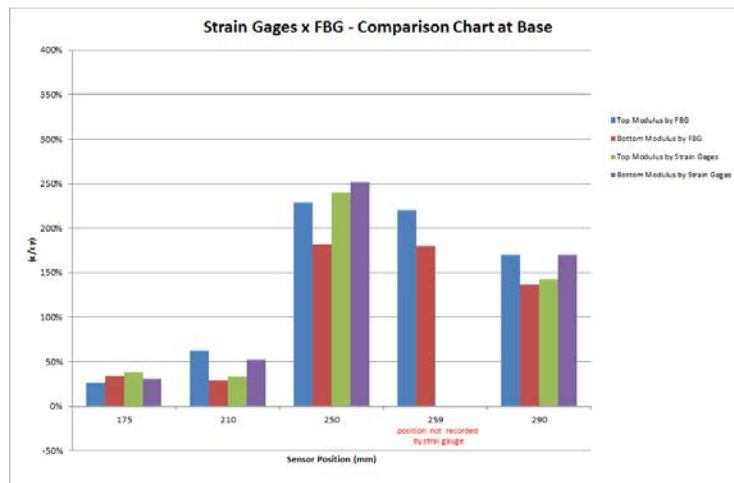


Figure 15 – Strain comparison between Strain Gage and FBG techniques base position.

The results presented in Figures 14 and 15 show almost the same reliability. Strain gages are less expensive than FBG, with around 20 times less being spent on strain gages than was spent on FBG. The epoxy adhesive used for the FGB sensors performed better than the cyanoacrylate adhesive used for the strain gages, though epoxy adhesive can also be utilized for strain gages. It is important to note that epoxy adhesive requires a curing process. During the strain gage tests some were lost when the strains reached high levels. This was a result of the difficulty in choosing the correct adhesive parameters for the strain levels and as a result some tests needed to be repeated.This did not occur in the FBG tests where all sensors were measured during the entire test without loss of any fiber. Both techniques took almost the same length of time to perform the installation, test and data analyses.

## 5. CONCLUSION

Based on the above data, it can be concluded that the test methodology used in these tests presents coherent results in detecting the high residual strains introduced into the tensile armor during manufacture, which can significantly impact the fatigue life of the tensile armors. This comparison shows the necessity of increasing the radius during the pipe end fitting processes to reduce the residual strains generated by the bending of the tensile armors.

## 6. ACKNOWLEDGEMENTS

## 7. REFERENCES

Antunes, P.F.C., 2010, "Análise dinâmica de estruturas com sensores de Bragg" – Master degree dissertation.

Classroom notes, 2013, "Fiber Optical Sensors". Pontifícia Universidade Católica – PUC-Rio.

Quintero, S.M.M. et al, 2005 - Thin film stress measurement by fiber optic strain gage, Thin Solid Films, 494, 141-145.

Cunha, J.R.F.A, 2007 –"Modelo Teórico de Sensores Ópticos Baseados em Fibras com Grade de Bragg" – Master degree dissertation.

Grattan, K.T.V., Meggitt, B.T. (Eds.), 1995, Optical Fiber Sensor Technology, Champman and Hall, London.

Lopes, D.G, 2013, "Avaliação das Tensões Residuais Provenientes do Processo de Montagem de Conectores em Armaduras de Tração de Dutos Flexíveis", On going Master Degree Dissertation, Rio de Janeiro, CEFET/RJ.

Santos, F. P, Lopes, D. G., 2008, "Projeto de um dispositivo para ensaio de fadiga de armaduras de tração de dutos flexíveis em ambiente corrosivo". Undergraduate Project. Centro Federal de Educação Tecnologia – Celso Suckow da Fonseca CEFET/RJ, Rio de Janeiro, Brazil.

Sheldrake,T., 2008, "Development of the End Fitting Tensile Wires Fatigue Analysis Model: Sample Tests and Validation in an Unbonded Flexible Pipe", OTC 1997.

Vargas, F.A, 2013 "Avaliação das Tensões Residuais em Armaduras de Tração de Dutos Flexíveis pelo Método Experimental da Rede de Bragg", On going Master Degree Dissertation, Rio de Janeiro, CEFET/RJ.

Xavier, Flávio Galdino, 2009 "Avaliação da vida em fadiga de um novo modelo de terminal conector para dutos flexíveis", Philosophy Doctor Thesis, - Rio Grande do Sul, UFRGS, Porto Alegre, Brazil.

## 7. RESPONSIBILITY NOTICE